

NASA LAW, February 14-16, 2006, UNLV, Las Vegas

Sensitivity Analysis Applied to Atomic Data Used for X-ray Spectrum Synthesis

T. Kallman

NASA/GSFC, Code 662, Greenbelt, MD 20771

1. Introduction

A great deal of work has been devoted to the accumulation of accurate quantities describing atomic processes for use in analysis of astrophysical spectra. But in many situations of interest the interpretation of a quantity which is observed, such as a line flux, depends on the results of a modeling- or spectrum synthesis code. The results of such a code depends in turn on many atomic rates or cross sections, and the sensitivity of the observable quantity on the various rates and cross sections may be non-linear and if so cannot easily be derived analytically. This paper describes simple numerical experiments designed to examine some of these issues. Similar studies have been carried out previously in the context of solar UV lines by Gianetti et al. (2000); Savin & Laming (2002) and in the context of the iron M shell UTA in NGC 3783 by Netzer (2004).

We perturb the dielectronic recombination (DR) rates according to the prescription:

$$\log(\text{Rate}') = \gamma \log(\text{Rate}) \quad (1)$$

where the constant γ is a randomly distributed quantity in the range $0.9 \leq \gamma \leq 1.1$. It is randomly chosen for each ion, but is the same for a given ion at all temperatures. The remainder of this paper is devoted to exploring the results of this experiment for gases in both coronal and photoionization equilibrium, and the consequences for the results derived from fitting to recent data from the Chandra X-ray telescope. In addition, we also examine briefly the effects of factor ~ 2 changes in the rates of ionization by the Auger mechanism, for photoionized plasmas.

2. Coronal ionization balance

Figure (1) shows the ionization balance for gas assuming coronal equilibrium. The left panel shows the ionization balance of iron calculated using the rates equivalent to the rates compiled by Arnaud & Raymond (1992) for dielectronic recombination (DR) and electron

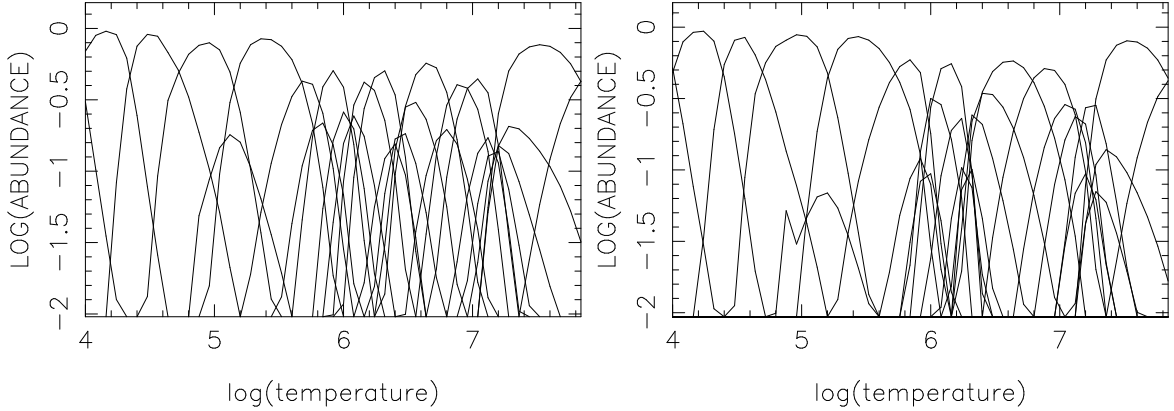


Fig. 1.— Coronal ionization balance for iron using baseline (left) and perturbed (right) recombination rates

impact collisional ionization. The right panel shows the ionization balance obtained when the same DR rates are randomly perturbed using the prescription given in the previous section. This shows that perturbing the DR rates by the amount chosen here leads to a change in the temperature where the abundance of a given ion peaks of $\Delta \log(T)=0.1$ for some ions, and less for stable ions such as Fe^{16+} .

3. Coronal Fitting Results

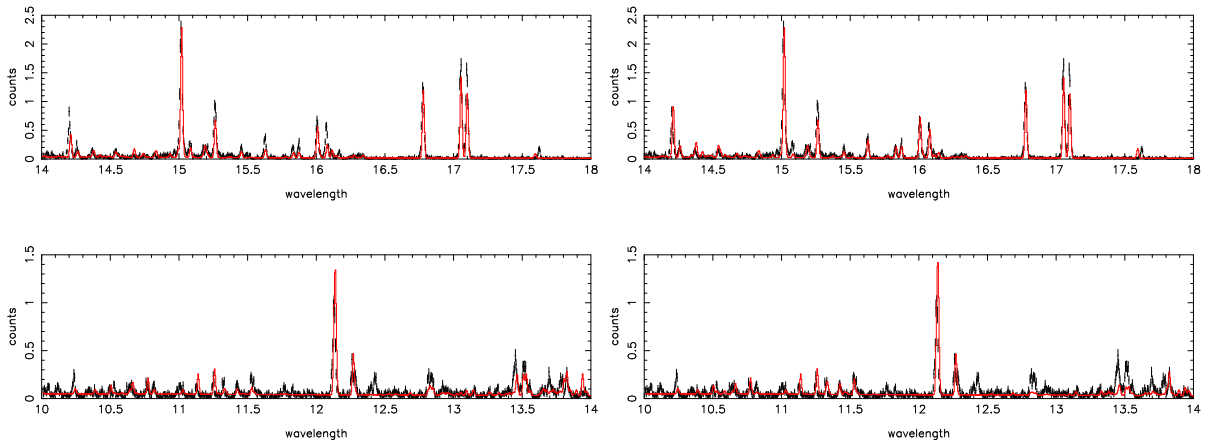


Fig. 2.— Fit to HETG Capella Spectrum using baseline ionization balance (left) and perturbed ionization balance (right)

Figure (2) shows a fit of coronal emission model to a 60 ksec Chandra HETG observation of the active star Capella, similar to that reported by Canizares et al. (2000). The left panels show a fit of the Chandra data to a model calculated using the baseline ionization

balance from Figure (1). The solid (red) curve shows a fit of 2 component model, with $\log(T)=6.9,7.1$. The χ^2 for this fit is 3267 for 1602 degrees of freedom. The abundances are $[\text{Ne}/\text{Fe}]=2.1$, $[\text{O}/\text{Fe}]=1$. The right panels show a fit using the ionization balance calculated using the perturbed DR rates shown the right panel of figure (1). With no attempt at iterative improvement this gives $\chi^2=3610/1602$. When this model is iteratively fit to the data $\chi^2=3522/1602$ which is still inferior to the baseline model, and the derived temperatures are: $\log(T)=6.9,7.2$.

4. Photoionized ionization balance

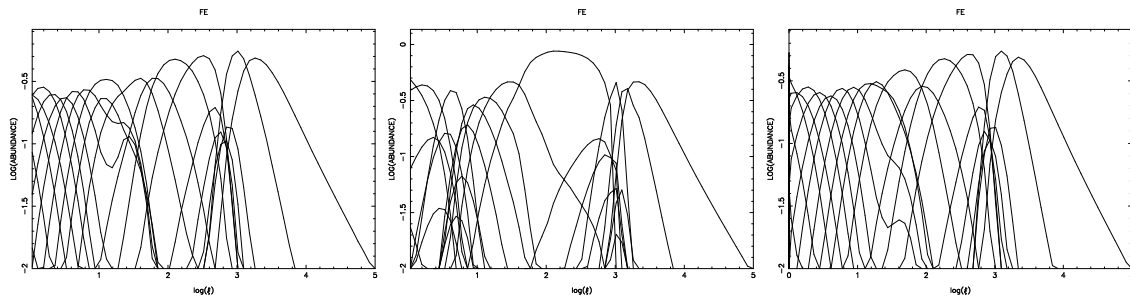


Fig. 3.— Photoionized ionization balance, baseline (left), using perturbed DR (center), and doubled K shell photoionization (right).

Figure (3) shows the ionization balance for gas assuming photoionization equilibrium, assuming a power law ionizing spectrum with energy index 1. The left panel shows the ionization balance of iron calculated using the rates described by Bautista & Kallman (2001) as implemented in the xstar code (Kallman & Bautista 2001). The middle panel shows the ionization balance obtained when the same randomly perturbed dielectronic recombination rates are used as were used in figures 1 and 2. The right panel shows the ionization balance obtained when the K shell photoionization rates are doubled. Since K shell ionization leads to multiple ionization via the Auger mechanism a significant fraction of the time, this is tantamount to a doubling of the Auger ionization rate. The middle panel shows that perturbing the DR rates has a greater effect in the photoionized case, and leads to a change in the ionization parameter where the abundance of a given ion peaks of $\Delta \log(\xi)=0.2$ or greater. Increasing the Auger rate in this case has a smaller effect, $\Delta \log(\xi)=0.1$.

5. Photoionized Fitting results

Figure (4) shows a small portion of a fit of photoionization model to the 900 ksec Chandra HETG observation of NGC 3783 first reported by Kaspi et al. (2001, 2002). The solid (red) curve shows a fit of 2 component photoionization model, with $\log(\xi)=2.2, 0.1$. The χ^2

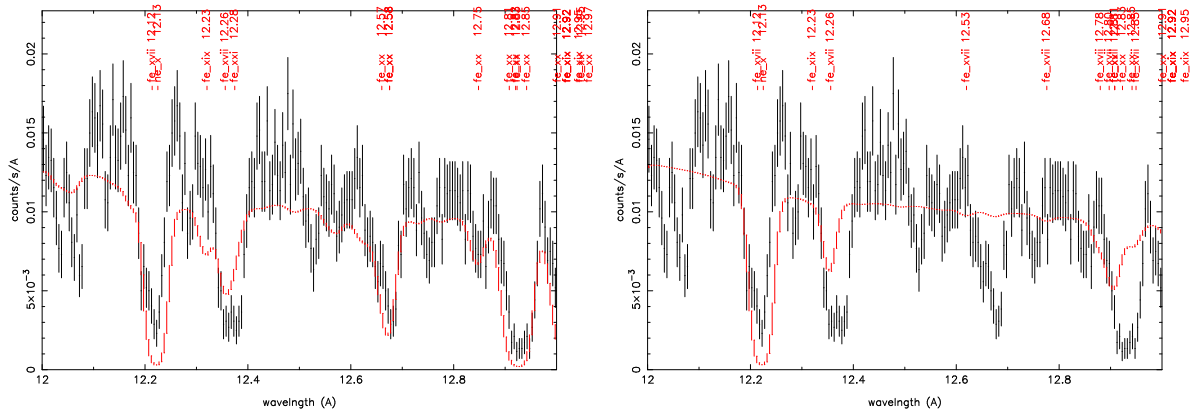


Fig. 4.— Fit of 2 component warm absorber model to the 900 ksec Chandra HETG observation of NGC 3783 in the 12-13 Å region. Xstar model using baseline (DR) rates (left) and using perturbed DR rates (right).

for this fit (including the entire HETG band) is 11105 for 8192 degrees of freedom. The model is calculated using the xstar code (Kallman & Bautista 2001) including recent compilations of the line energies and oscillator strengths for lines of iron by the Chianti collaboration (Landi et al. 2006). An blueshift of 700 km/s and a turbulent velocity of 300 km/s were assumed. The elemental abundances are $[\text{Ne}/\text{O}]=1$, $[\text{Si}/\text{O}]=1$, $[\text{S}/\text{O}]=2$, $[\text{Fe}/\text{O}]=0.4$. These parameters are similar to those derived by Krongold et al. (2003).

Comparison between the fit to the NGC 3783 using the baseline ionization balance and that obtained using the perturbed DR rates is shown in figure (4). With no iterative improvement this gives $\chi^2=17660/8192$. The figure shows the fit when this model is iteratively fit to the data. The χ^2 is 13072/8192, which is still inferior to the baseline model, and the derived ionization parameters are $\log(\xi)=2.9, 0.1$. This is significantly different from that obtained with the baseline model.

6. Conclusions

We have shown that changes in the DR rates of ~ 0.1 in the logarithm of the rate lead to comparable changes in the ionization balance distribution with temperature in the coronal case. The results of fitting to high resolution X-ray data are affected by a comparable amount. In the photoionized case, the ionization balance is more strongly affected by the same changes in DR rates, leading to changes in $\log(\xi)$ of 0.2, and comparable changes in the conditions inferred from fitting. Definitive conclusions on the sensitivity of astrophysical results to DR rates, and other rates, require more extensive experimentation, including a large number of such random trials.

REFERENCES

- Arnaud, M., & Raymond, J. 1992, *ApJ*, 398, 39
- Bautista, M. A., & Kallman, T. R. 2001, *ApJS*, 134, 139
- Canizares, C. R., et al. 2000, *ApJ*, 539, L41
- Gianetti, D., Landi, E., & Landini, M. 2000, *A&A*, 360, 1148
- Kallman, T., & Bautista, M. 2001, *ApJS*, 133, 221
- Kaspi, S., et al. 2002, *ApJ*, 574, 643
- Kaspi, S., et al. 2001, *ApJ*, 554, 216
- Krongold, Y., Nicastro, F., Brickhouse, N. S., Elvis, M., Liedahl, D. A., & Mathur, S. 2003, *ApJ*, 597, 832
- Landi, E., Del Zanna, G., Young, P. R., Dere, K. P., Mason, H. E., & Landini, M. 2006, *ApJS*, 162, 261
- Netzer, H. 2004, *ApJ*, 604, 551
- Savin, D. W., & Laming, J. M. 2002, *ApJ*, 566, 1166
- Smith, R. K., Brickhouse, N. S., Liedahl, D. A., & Raymond, J. C. 2001, *ApJ*, 556, L91